ELECTROEXCITATION OF GIANT RESONANCES BETWEEN 5 MeV AND 30 MeV EXCITATION ENERGY IN ^{165}Ho

Gerald Lee Moore

NAVAL POSTGRADUATE SCHOOL
Monterey, California

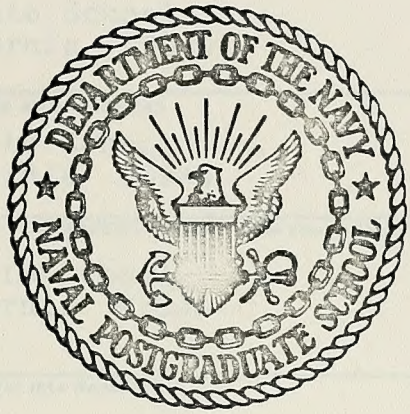

THESIS

ELECTROEXCITATION OF GIANT RESONANCES
BETWEEN 5 MeV AND 30 MeV
EXCITATION ENERGY IN ^{165}Ho

by

Gerald Lee Moore

December 1974

Thesis Advisors: F. R. Buskirk
X. K. Maruyama

Approved for public release; distribution unlimited.

UNCLASSIFIED

SECURITY CLASSIFICATION OF THIS PAGE (When Data Entered)

REPORT DOCUMENTATION PAGE		READ INSTRUCTIONS BEFORE COMPLETING FORM
1. REPORT NUMBER	2. GOVT ACCESSION NO.	3. RECIPIENT'S CATALOG NUMBER
4. TITLE (and Subtitle) Electroexcitation of Giant Resonances Between 5 MeV and 30 MeV Excitation Energy in ^{165}Ho		5. TYPE OF REPORT & PERIOD COVERED Master's Thesis; December 1974 6. PERFORMING ORG. REPORT NUMBER
7. AUTHOR(s) Gerald Lee Moore		8. CONTRACT OR GRANT NUMBER(s)
9. PERFORMING ORGANIZATION NAME AND ADDRESS Naval Postgraduate School Monterey, California 93940		10. PROGRAM ELEMENT, PROJECT, TASK AREA & WORK UNIT NUMBERS
11. CONTROLLING OFFICE NAME AND ADDRESS Naval Postgraduate School Monterey, California 93940		12. REPORT DATE December 1974 13. NUMBER OF PAGES 63
14. MONITORING AGENCY NAME & ADDRESS(if different from Controlling Office) Naval Postgraduate School Monterey, California 93940		15. SECURITY CLASS. (of this report) Unclassified 15a. DECLASSIFICATION/DOWNGRADING SCHEDULE

16. DISTRIBUTION STATEMENT (of this Report)

Approved for public release; distribution unlimited.

17. DISTRIBUTION STATEMENT (of the abstract entered in Block 20, if different from Report)

18. SUPPLEMENTARY NOTES

19. KEY WORDS (Continue on reverse side if necessary and identify by block number)

Inelastic electron scattering
Giant resonances
Multipole transitions
Nuclear resonances
Nuclear transitions
LINAC
Holmium isotope 165

20. ABSTRACT (Continue on reverse side if necessary and identify by block number)

Giant resonances in ^{165}Ho were studied with inelastic scattering of electrons with 60 MeV to 105 MeV incident energy at a scattering angle of 75 degrees. From 5 MeV to 30 MeV excitation energy, five multipole resonances were observed of which only the dipole resonances have been previously reported. Reduced transition probabilities and multipolarity assignments have been made. The five

DD FORM 1 JAN 73 1473 (Page 1) EDITION OF 1 NOV 65 IS OBSOLETE S/N 0102-014-6601 |

UNCLASSIFIED

SECURITY CLASSIFICATION OF THIS PAGE (When Data Entered)

Block #20 Continued

resonances were observed at excitation energies of 9.6 (E0 or E2), 11.5 (E2), 12.3 (E1), 15.8 (E1), and 23.5 MeV (E2). The splitting of the dipole resonance observed in photonuclear reaction experiments with prolate spheroid nuclei are confirmed with inelastic electron scattering.

Electroexcitation of Giant Resonances Between 5 MeV and 30 MeV Excitation Energy in ^{165}Ho

by

Gerald Lee Moore
Lieutenant, United States Navy
B.S., Texas A&M University, 1968

Submitted in partial fulfillment of the
requirements for the degree of

MASTER OF SCIENCE IN PHYSICS

from the

NAVAL POSTGRADUATE SCHOOL
December 1974

ABSTRACT

Giant resonances in ^{165}Ho were studied with inelastic scattering of electrons with 60 MeV to 105 MeV incident energy at a scattering angle of 75 degrees. From 5 MeV to 30 MeV excitation energy, five multipole resonances were observed of which only the dipole resonances have been previously reported. Reduced transition probabilities and multipolarity assignments have been made. The five resonances were observed at excitation energies of 9.6 (E0 or E2), 11.5 (E2), 12.3 (E1), 15.8 (E1), and 23.5 MeV (E2). The splitting of the dipole resonance observed in photonuclear reaction experiments with prolate spheroid nuclei are confirmed with inelastic electron scattering.

TABLE OF CONTENTS

LIST OF TABLES

LIST OF FIGURES

ACKNOWLEDGEMENTS

This thesis is a result of the encouragement, guidance, and many hours of assistance provided by my Thesis Advisors, Professor Fred R. Buskirk, Professor Xavier K. Maruyama, and visiting Professor W. Rainer Pitthan. I can only describe my special thanks and appreciation by acknowledging my total indebtedness to them.

Thanks are also extended to Professor John N. Dyer for his assistance during the long hours of data collection and Professor E. B. Dally for his assistance by preparing the target samples.

I. INTRODUCTION

Giant resonance investigations using the 120 MeV electron linear accelerator of the Naval Postgraduate School have been conducted since 1973. The previous work has been with ^{197}Au and ^{208}Pb [Refs. 1, 2, and 3]. The data reduction techniques necessary to cope with the large bremsstrahlung background, called the radiation tail, has been greatly improved from the initial attempts. Using computer codes and techniques originally developed at Darmstadt and reported by Buskirk, *et. al.*, [Ref. 4] it has been possible to determine giant resonances of different multipolarities and to make model comparisons with the experimental evidence.

The previous work at the Naval Postgraduate School facility on gold and lead were done at various values of momentum transfer, most commonly at a fixed machine energy and at varying scattering angles. The investigation eventually covered an excitation range of 5 MeV to 40 MeV. It was desired to determine if similar information could be achieved by fixing the scattering angle and varying the momentum transfer by using different incident energy electrons. It was decided to study the inelastic electron scattering spectra of ^{165}Ho in the same energy range for three reasons. First, holmium, which is easily obtained in a isotopically pure form, has a deformed nucleus with a relatively large intrinsic quadrupole moment. Scattering from this isotope should illustrate several predicted features

unique to deformed nuclear structure. Second, this element has been well reported in the literature [Refs. 5, 6, 7, 8, 9, 10, 11, 12, and 13], particularly the study of giant resonances by photoneutron experiments. Since these works dealt primarily with the giant dipole resonance, it was advantageous to study other multipolarities using the technique of inelastic electron scattering. Third, only the elastic electron scattering from ^{165}Ho has been studied by Safrata, *et. al.*, [Ref. 8] and Uhrhane, *et. al.*, [Ref. 12].

Foil samples of ^{165}Ho were prepared and four experiments were done at a scattering angle of 75 degrees. Using transmission geometry, data were collected with incident electrons of 60, 75, 90 and 105 MeV energy. The momentum transfer squared thus achieved ranged from 0.137 fm^2 to 0.420 fm^2. Experimental values of the inelastic form factors were determined from the data and transition multipolarities were assigned to five observed giant resonances. Three resonances of excitation energy 9.6, 11.5, and 23.5 MeV are reported here for the first time. Comparisons between surface oscillations, Goldhaber-Teller model [Ref. 14] and volume oscillations, Steinwedel-Jensen model [Refs. 15 and 16] were also made.

There were three objectives of this research. The first was to determine if the multipolarities of giant resonances could be assigned by measuring inelastic scattering form factors as a function of incident electron energy rather than the scattering angle as has been done in the past at this facility [Refs. 1 and 2]. Second, inelastic electron

scattering could be used to investigate multipolarity and isospin assignment of the observed giant resonance of the ^{165}Ho nucleus. Third, the splitting of the giant dipole resonance is observed in the photoneutron reactions in ^{165}Ho and it was desirable to explore the possibility of similar splitting of the quadrupole transitions.

II. THEORY

A. ELECTRON SCATTERING EXPERIMENTATION

The electromagnetic interaction between the electron and the nucleus is well understood and is composed of Coulomb interactions between charges and the current and magnetic moment interactions of the nucleus with the electromagnetic field of the passing electron. All these interactions are described by the physical theories of quantum electrodynamics and hence are known well enough to make exacting predictions. As a consequence, an analysis of electron scattering data directly produces information on the target nucleus itself, without any details of the imperfectly known strong interactions interfering in the analysis, such as is the case in nuclear structure studies with heavy particle reactions.

There are two other main possibilities of using electromagnetic interactions for studying nuclear structure, nuclear absorption and scattering of photons and Coulomb excitation by heavy, charged particles. These have disadvantages when compared with inelastic electron scattering. Photons cannot be utilized to determine ground state information since the momentum transfer $\underset{\sim}{q}$ is determined uniquely by the nuclear excitation, ω. Electron scattering does not restrict the experimentalist in this respect. For electron scattering the momentum transfer can be varied through a wide range of values since it is given by the expression

$$\underset{\sim}{q} = \underset{\sim}{k}_1 - \underset{\sim}{k}_2 \qquad \text{(II-1)}$$

where $\underset{\sim}{q}$ is the four vector momentum-energy transfer and $\underset{\sim}{k}_1$ and $\underset{\sim}{k}_2$ are respectively the four vector incident and scattered electron momenta. The magnitude of $\underset{\sim}{q}$ transferred to the nucleus is dependent only on the incident and scattered electron energies and the scattering angle by the relation [Ref. 16]

$$q^2 = - 4 E_i E_f \sin^2(\theta/2) \qquad \text{(II-2)}$$

for highly relativistic electrons. Since q can be varied for constant excitation energy of the nucleus, $E_x = E_i - E_f$, momentum analysis of the scattered electrons may reveal excitations not previously observed in photonuclear work. Coulomb excitation, using the electric field of heavy, charged particles, has the same advantages as mentioned above for the electron. However, these experiments are limited in that magnetic transitions are very difficult to excite and the energy of the incident charged particles must be limited to less than the Coulomb barrier energy.

In the first order Born approximation for electron scattering the electrons can be considered to be relativistic Dirac particles scattered from massive point nuclei as was done by Mott [Ref. 17]. The incident particle, the electron, is assumed to have a spin and a Dirac magnetic moment, although the scattering center is assumed to have neither spin nor a magnetic moment. The resulting differential cross section for scattering is thus given by

$$(d\sigma/d\Omega)_{Mott} = \left[\frac{Z e^2}{2E_i}\right]^2 \frac{\cos^2(\theta/2)}{\sin^4(\theta/2)} \qquad \text{(II-3)}$$

for highly relativistic electrons. For a nucleus of finite size a quantity determined by the nuclear structure must be included. The measured differential cross section becomes

$$(d\sigma/d\Omega)_{measured} = (d\sigma/d\Omega)_{Mott} \cdot \left| \int_{\text{nuclear volume}} \rho(\vec{r}) e^{i\vec{q}\cdot\vec{r}} \, d\tau \right|^2 . \qquad \text{(II-4)}$$

The factor multiplying the Mott cross section is the "structure factor" or "form factor" analogous to electron and x-ray diffraction studies, and is in fact called the nuclear form factor. It is usually this term which is determined in elastic scattering experiments from calculated Mott cross sections and measured elastic cross sections. This yields the nuclear form factor

$$|F(q^2)|^2 = (d\sigma/d\Omega)_{elastic} \; / \; (d\sigma/d\Omega)_{Mott} . \qquad \text{(II-5)}$$

B. INELASTIC ELECTRON SCATTERING

Analytical expressions for the differential cross section for inelastic electron scattering may be derived in a manner similar to that for the elastic cross sections using the plane wave Born approximations. In this approximation the differential cross section $(d\sigma/d\Omega)_{PWBA}$ for nuclear excitation by inelastic electron scattering can be written as a sum over the separate cross sections for electric and magnetic multipole transitions.

$$(d\sigma/d\Omega)_{PWBA} = \sum_{\lambda} (\partial\sigma/\partial\Omega)_{E\lambda} + \sum_{\lambda} (\partial\sigma/\partial\Omega)_{M\lambda}. \qquad \text{(II-6)}$$

The electric multipole terms are given by Theissen [Ref. 18]

$$(d\sigma/d\Omega)_{E\lambda} = \alpha^2 a_\lambda q^{2\lambda} k_o^{-2} \left[\lambda(\lambda+1)^{-1} B(C\lambda,q) V_L(\theta) + B(E\lambda,q) V_T(\theta)\right] R^{-1} \qquad \text{(II-7)}$$

and those of the magnetic multipoles by a similar expression

$$(d\sigma/d\Omega)_{M\lambda} = \alpha^2 a_\lambda q^{2\lambda} k_o^{-2} B(M\lambda,q) V_T(\theta) R^{-1}. \qquad \text{(II-8)}$$

In these equations

$$a_\lambda = 4\pi\lambda^{-1}(\lambda+1)[(2\lambda+1)!!]^{-2}$$

$$k_o = E_o/hc$$

$$R = 1 + hc(k_o/Mc^2)(1-\cos\theta)$$

with the following definitions of the terms

λ - transition multipolarity

α - fine structure constant

E_o - incident electron energy

θ - scattering angle

M - nuclear mass.

The factor R takes into account the effect of the recoiling nucleus on the final state density. The functions $V_L(\theta)$ and $V_T(\theta)$ account for the longitudinal and traverse components of the four vector nucleus current density resolved into components parallel and perpendicular respectively to the three vector momentum transfer $\vec{q}$. The component parallel to $\vec{q}$ corresponds to an interaction of the electron with the

nuclear charge, whereas the perpendicular component is a contribution from the nuclear current and magnetization densities. For E_o large compared to the electron rest energy the functions $V_L(\theta)$ and $V_T(\theta)$ are defined by Theissen [Ref. 18] to be

$$V_L(\theta) = \tfrac{1}{2}(1+\cos\theta) \; / \; (y-\cos\theta)^2 \qquad \text{(II-9)}$$

$$V_T(\theta) = \tfrac{1}{4}(2y+1-\cos\theta) \; / \; (y-\cos\theta)(1-\cos\theta) \qquad \text{(II-10)}$$

with $y = 1 + E_x^2 \; / \; 2E_o(E_o - E_x)$ and E_x the excitation energy. For a scattering angle of 75 degrees both $V_L(\theta)$ and $V_T(\theta)$ are approximately one. The quantities $B(^{E}_{M}\lambda,q)$ represent the reduced nuclear transition probabilities which will be described in a later section.

In the plane wave Born approximation (PWBA) the incoming and outgoing electrons are described by plane waves. If the charge is large such that $Z\alpha$ is not much less than unity, the electron field is distorted and can no longer be modeled by a plane wave. In this case the electron wave functions are used which are solutions to the Dirac equation in the presence of a field due to the static ground state charge distribution of the target nucleus. This model is called the distorted wave Born approximation, DWBA, since the effect of the nuclear charge on the wave function of the electron is to distort both the incident and scattered electron wave functions in a manner such that a plane wave solution no longer yields satisfactory results. In practice, the plane wave solutions of the PWBA are replaced by phase

shifted spherical waves which require computer computations and the concept of form factor loses its simple meaning [Ref. 19].

C. NUCLEAR MODELS

In this work the models of the nuclear transition charge density as introduced by Goldhaber and Teller [Ref. 14] and by Steinwedel and Jensen [Ref. 15] were tested against the data for comparison and transition strength determinations. A brief description of these models and how they are incorporated into the distorted wave Born approximation calculations for the inelastic form factors is given here.

The generalized Goldhaber-Teller model as described by Überall [Ref. 16] for any multipolarity assumes the nucleus to consist of four interpenetrating fluids, protons with either spin up ($\uparrow$) or spin down ($\downarrow$) and similar states for the neutrons. Any two of these states oscillating 180 degrees out of phase against the other two gives rise to three possible collective modes. The original discussion by Goldhaber and Teller [Ref. 14] thus corresponds to protons, ($p\uparrow$, $p\downarrow$), oscillating against neutrons, ($n\uparrow$,$n\downarrow$). Other possibilities are ($p\uparrow$,$n\uparrow$) against ($p\downarrow$,$n\downarrow$) and ($p\uparrow$,$n\downarrow$) against ($p\downarrow$,$n\uparrow$). An oscillation of all four fluids in phase may produce a fourth, compressional mode. It requires the nuclear matter to be compressible in a monopole vibration.

In the Goldhaber-Teller model the charge density of the ground state $\rho_o(r)$ is assumed to be displaced rigidly such that the charge density becomes

$$\rho(r) = \rho_o(r) - \tfrac{1}{2}\,\vec{d}\cdot\nabla\rho_o(r) \qquad \text{(II-11)}$$

where the displacement vector $\vec{d}$ between the centers of the neutron and the proton spheres is small. This then describes the dipole motion. Überall [Ref. 16] shows that this may be further generalized to multipole motion if the ground state density is assumed to be deformed by a scale factor η such that the charge density becomes

$$\rho(r) = \rho_o(r) + \rho_{tr}(r) \qquad \text{(II-12)}$$

with the transition charge density

$$\rho_{tr}(r) = -\eta\, r\, \left(\frac{d\,\rho_o(r)}{dr} \right). \qquad \text{(II-13)}$$

The scale factor itself is then expanded in a multipole series

$$\eta = \sum_{\ell m} \alpha_{\ell m}\, (r/R)^{\ell + k_\ell - 2}\, Y_{\ell m}(\theta,\phi) \qquad \text{(II-14)}$$

with $k_\ell = 2\delta_{\ell o}$ (where $\delta_{\ell o}$ is the Knonecker delta). R is a reference radius given to make η dimensionless. A similar multipole expansion is possible for the current and magnetization densities.

For the Steinwedel and Jensen model a collective motion of the neutrons and protons is still assumed but the changes are brought about by shifts in the relative densities of the two fluids bounded by a rigid nuclear surface of radius R. As described by Überall [Ref. 16] this requires the charge density to be modeled by

$$\rho(r) = \rho_p(r) + \rho_n(r) = \text{constant} \qquad \text{(II-15)}$$

for $r \leq R_o$ with $R_o = 1.2\ A^{1/3}$. Again a scale factor is introduced such that

$$\rho_p(\vec{r},t) = \frac{Z}{A}\rho_o + \eta(\vec{r},t) \qquad \text{(II-16)}$$

$$\rho_n(\vec{r},t) = \frac{N}{A}\rho_o - \eta(\vec{r},t). \qquad \text{(II-17)}$$

As the nuclear surface is assumed to be rigid there can be no outflow through the surface hence

$$(\partial\eta/\partial r)_{r=R_o} = 0 \qquad \text{(II-18)}$$

and again η is expanded in a multipole form.

These transition densities may then be translated into theoretical form factors by using the expression of Ziegler [Ref. 19]

$$|F(q)|^2 = \frac{4\pi}{Z^2}\left(\frac{\lambda+1}{\lambda}\right)\frac{q^2}{(2\lambda+1)!!}^2 B(^{E}_{M}\lambda,q) \qquad \text{(II-19)}$$

for the transverse (E) and magnetic (M) components. A similar expression can be written for the longitudinal components. The coefficients, $B(^{E}_{M}\lambda,q)$, are the reduced nuclear transition probabilities mentioned before. Alder, *et. al.*, [Ref. 20] defines the transition probabilities by the relation

$$B(\lambda,J_i\rightarrow J_f) = \frac{1}{2J_i+1}\,|\langle J_f||M(\lambda,q)||J_i\rangle|^2 \qquad \text{(II-20)}$$

where the operator M represents the particular transition type and J_i and J_f the initial and final angular momentum of the nucleus, respectively. Zeigler [Ref. 19] develops the representation of these operators using the plane wave Born approximation for Coulomb (longitudinal) interactions,

$$M(C\lambda,q) = \frac{(2\lambda+1)!!}{q^{\lambda}} \int \rho_{tr} j_{\lambda}(qr) Y_{\lambda m}(\theta,\phi) d\tau, \qquad \text{(II-21)}$$

for the electric part of the transverse interaction

$$M(E\lambda,q) = \frac{(2\lambda+1)!!}{q^{\lambda+1}(\lambda+1)} \int \hat{j}_n \nabla \cdot \hat{L}[j_{\lambda}(qr) Y_{\lambda m}(\theta,\phi)] d\tau \qquad \text{(II-22)}$$

and for the magnetic part of the transverse interaction

$$M(M\lambda,q) = -i \frac{(2\lambda+1)!!}{q^{\lambda}(\lambda+1)} \int \hat{j}_n \cdot \hat{L}[j_{\lambda}(qr) Y_{\lambda m}(\theta,\phi)] d\tau \qquad \text{(II-23)}$$

where $\hat{j}_n$ is the nuclear current operator as defined by the particular model, $\hat{L}$ is the orbital momentum operator, and $j_{\lambda}(qr)$ is the spherical Bessel function of order λ. Following the development of Überall [Ref. 16] the reduced transition probabilities become in the plane wave Born approximation,

$$B(\begin{matrix}E\\M\end{matrix}\lambda,q) = (\lambda+1)\frac{[(2\lambda+1)!!]^2}{q^{2\lambda}} \left| \int j_{\lambda}(qr) \rho_{tr}(r) d\tau \right|^2 . \qquad \text{(II-24)}$$

The model dependent inelastic form factors are calculated using the distorted wave Born approximation in the computer code GBROW described by Zeigler [Ref. 19]. The reader is also referred to the discussion by Überall [Ref. 16] particularly Section 6.4. In this particular code the transition probabilities are normalized to unity. To determine the strength of the observed transitions it is thus necessary to calculate the magnitude of the theoretical form factors which would give similar results as the measured form factors. The average of the strenghs determined for each

experiment is then taken as an estimate of the observed transition strengths. The B values thus determined are then used to compare the theoretical inelastic form factors with the experimental values to determine a best fit to the data points. This final B value is then reported as the observed strength of the resonance.

To determine whether or not the observed resonances are collective phenomena, comparison of experimental to single-particle reduced transition probabilities may be made. The ratio of these values would be expected to be significantly greater than one for the giant multipole resonances. Furthermore, a giant resonance should exhaust an appreciable fraction of the appropriate sum rule. If an observed resonance greatly exceeds the sum rule under the assumption of a particular transition, it is unlikely that the multipolarity assignment is correct.

The single-particle reduced transition strengths are given in Weisskopf units [Ref. 21]

$$B(E\lambda)_{SPU} = \frac{e^2(2\lambda+1)}{4\pi} \left(\frac{3}{\lambda+3}\right)^2 R^{\lambda} \qquad \text{(II-25)}$$

and

$$B(M\lambda)_{SPU} = \frac{e^2(2\lambda+1)}{\pi} \left(\frac{3}{\lambda+3}\right)^2 R^{2\lambda-2} (0.0111) \qquad \text{(II-26)}$$

where $R_o = 1.2\ A^{1/3} = 6.47$ fm for ^{165}Ho.

Another, to some extent model independent, evaluation of the transition strength of Eλ modes may be achieved by expressing the strength relative to the energy weighted sum

rule (EWSR). Sum rules for the magnetic transitions are more dependent upon the current and magnetic moment distributions of the nucleus and hence are more model dependent. Because of these limitations and since magnetic transition strengths are very small at forward angles, they are not presented here. The sum rule for isoscalar ($\Delta T=0$) excitation modes with $L>1$ is given by Nathan and Nilsson [Ref. 22],

$$S(E\lambda, T=0) = \sum_f (E_f - E_i) B(E\lambda, q) = \frac{Z^2 e^2 \lambda (2\lambda+1)^2 h^2 \langle R^{2\lambda-2} \rangle}{8\pi A M_p} . \quad \text{(II-27)}$$

The isovector ($\Delta T=0$) sum rule for $L>1$ is related to the isoscalar sum rule by

$$S(E\lambda, \Delta T=1) = S(E\lambda, \Delta T=0) \frac{N}{Z} . \quad \text{(II-28)}$$

The corresponding sum rule for an isoscalar monopole (E0) excitation is given by Ferrell [Ref. 23]

$$S(E0) = \sum_f (E_f - E_i) |M_{fi}|^2 = \frac{h^2 Z}{M_p} \langle R^2 \rangle \quad \text{(II-29)}$$

where M_{fi} is the monopole matrix element. The strength of E1 resonances can be expressed relative to the sum rule given by Warburton and Weneser [Ref. 24]

$$S(E1) = \frac{9 e^2 h^2}{8\pi M_p} \frac{NZ}{A} . \quad \text{(II-30)}$$

Table I gives values of the energy weighted sum rule (EWSR) and the single particle transition strengths for ^{165}Ho.

D. GIANT RESONANCE PHENOMENA

From the study of nuclear level structure by photonuclear processes, it is apparent that there is a collective feature of the nuclear excitation spectrum called the "giant resonance." The term was used initially to describe what is now recognized as the giant electric dipole resonance (GDR). In their original paper proposing that these features were indeed resonance structures, Goldhaber and Teller by inference also raised the possibilities that giant resonances existed with other multipolarities. Experimental evidence now indicates that these different order multipolarity resonance phenomena do in fact exist.

Early attempts to explain the giant dipole resonance were based mainly on collective models. The initial work by Goldhaber and Teller [Ref. 14] mentioned previously assumed that the protons and neutrons behave as two interpenetrating incompressible fluids. Using a strictly classical approach, the two fluids are considered to be relatively displaced during dipole oscillations such that the proton and neutron fluids no longer overlap near the surface. If the restoring force is assumed proportional to the surface area, or to R^2, then the frequency of the resulting harmonic motion is proportional to the square root of the force divided by the mass, or $\omega \sim (R^2/R^3)^{\frac{1}{2}} \sim R^{-\frac{1}{2}}$. Since $R \sim A^{1/3}$, then the resulting energy of the harmonic oscillator should be $E(GDR) \sim A^{-1/6}$. Goldhaber and Teller [Ref. 14] found the relation to be roughly $40A^{-1/6}$. It

should be noted here that the original Goldhaber-Teller model does not allow for monopole transitions since the two fluids are considered incompressible and hence changes in relative density cannot occur. The development of the generalized Goldhaber-Teller model by Überall [Ref. 16] does make provisions for a monopole transition in the expansion of η in equation (II-13).

The Steinwedel and Jensen model as described by Danos [Ref. 25] and in Section II-B assumes a collective motion within a rigid boundary. The energy of the giant dipole transition is shown by Danos [Ref. 25] for the spherical nucleus to be

$$E(GDR) = \frac{2.08}{R} \left[\frac{8KNZ}{M^*A^2}\right]^{\frac{1}{2}} \qquad \text{(II-31)}$$

where M^* is an effective nucleon mass and K is the energy associated with the symmetry energy term of the semi-empirical mass formula. Since the nuclear radius is proportional to $A^{1/3}$ then $E(GDR) \sim A^{-1/3}$ for the Steinwedel-Jensen model. One selection of the variables as made by Hayward [Ref. 26] yields

$$E(GDR) = 80\ A^{-1/3} \text{MeV}. \qquad \text{(II-32)}$$

Since these collective models of the nucleus predict that the giant dipole resonance energy varies inversely with the radius, a natural consequence is that for deformed nuclei having two characteristic dimensions (prolate spheroids) the giant resonance should be a superposition of two resonances. Okamoto [Ref. 27] and Danos [Ref. 25] have

shown that the overall width of the dipole resonance is strongly correlated to the nuclear deformation as measured by the intrinsic quadrupole moment. According to Danos [Ref. 25] the connection between the resonance energies E_a and E_b and the lengths of the long and short axes a and b respectively is given by

$$\frac{E_b}{E_a} = 0.911 \frac{a}{b} + 0.089. \qquad \text{(II-33)}$$

For ^{165}Ho the higher energy resonance corresponding to charge oscillations along the two short axes of the prolate spheroid would then comprise two-thirds of the integrated cross section. If the width, Γ, of the total giant dipole resonance is independent of the energy, Danos [Ref. 25] has shown that the ratio of the heights of the separate peaks is related by

$$\frac{\sigma_a)_{max}}{\sigma_b)_{max}} = \frac{1}{2} . \qquad \text{(II-34)}$$

Hence, the strengths of the two components of the E1 resonance have the simple ratio 1:2, corresponding to the number of degrees of freedom.

In the earliest work with ^{165}Ho by Petree, *et. al.*, [Ref. 5] a single dipole resonance peak was reported at 14.5 MeV with a width of 7.5 MeV. Fuller and Hayward [Ref. 6] first observed the splitting of the GDR in ^{165}Ho. They reported peaks at 12.3 MeV and 16 MeV. Bramblett, *et. al.*, [Ref. 7] found the energies to be 12.10 MeV and 15.75

MeV with widths of 2.65 MeV and 4.4 MeV respectively. Bergère, *et. al.*, [Ref. 9] reported splitting of the dipole resonance at energies of 12.01 MeV and 15.59 MeV. The corresponding widths of the Lorentz shape fits were Γ = 2.52 MeV and Γ = 5.12 MeV. The same splitting as observed by Kelley, *et. al.*, [Ref. 10] was 12.32 MeV (Γ = 2.32 MeV) and 15.78 MeV (Γ = 5.04 MeV). With data taken from photoneutron interactions with oriented ^{165}Ho nuclei, Berman, *et. al.*, [Ref. 11] reported slightly different energies of 12.28 MeV (Γ = 2.57 MeV) and 15.78 MeV (Γ = 5.00 MeV). It can be shown from their data that the ratio of the observed relative transition strengths rather than the apparent integrated γ cross section of the two resonances is for the Saclay group 1.92 [Ref. 9], 2.04 for Kelley, *et. al.*, [Ref. 10] and for Berman, *et. al.*, [Ref. 11] 1.76.

Schiff [Ref. 28] developed an analysis of the inelastic electron scattering cross section contribution from the transition quadrupole moment. Ligensa, *et. al.*, [Ref. 29] have extended this work with the Steinwedel-Jensen model to include quadrupole multipolarity for deformed nuclei. They predict five main quadrupole resonances. The first experimental evidence of a giant quadrupole (E2) resonance below the dipole resonance was found in inelastic electron scattering experiments at Darmstadt [Ref. 30]. The Sendai group [Ref. 31] reported a quadrupole resonance in ^{208}Pb at 22 MeV. These results were confirmed at NPS [Ref. 3], in experiments with ^{208}Pb and ^{197}Au where E2 resonances were reported at

22.5 MeV and 23.0 MeV respectively. The lower E2 resonance at $E_x = 63\ A^{-1/3}$MeV is generally referred to as the isoscalar ($\Delta T=0$) and the higher resonance at $E_x = 130\ A^{-1/3}$ as the isovector ($\Delta T=1$) [Ref. 3]. The existence of the lower quadrupole resonance and the observed splitting of the E1 resonance in deformed nuclei makes the evaluation more difficult. If one or both of the E2 resonance and the lower E1 resonance are relatively wide and separated by only a few MeV then disentanglement of the several resonances may be impossible.

The possibility of a monopole (E0) transition was first reported in the ^{208}Pb and ^{197}Au study mentioned previously [Ref. 3]. A mass number dependence of $E_x = 53\ A^{-1/3}$ was found in the data fit analysis. A corresponding transition in ^{165}Ho has not been previously reported as photonuclear absorption cannot excite a monopole transition.

Multipolarity λ	ΔT	Sum Rule $S(E\lambda,\Delta T)$ $e^2 MeV\ fm^{2\lambda}$	Single Particle Strength $e^2\ fm^{2\lambda}$
0	0	7.63×10^4 [a]	
1	-		8.10
1	1	5.92×10^2	
2	-		3.18×10^2
2	0	6.16×10^4	
2	1	9.01×10^4	

[a]Units for the monopole transition matrix elements are MeV-fm^4

Table I. Sum Rules and Single Particle Transition Strengths for ^{165}Ho.

III. DATA ACQUISITION

A. EXPERIMENTAL PROCEDURES

It was felt necessary to choose an optimum scattering angle which would disentangle the broad resonance structures of the giant multipole transitions DWBA calculations of the inelastic form factors for E1 and E2 transitions in ^{165}Ho were made using the computer code GBROW [Ref. 19]. Both volume and surface oscillation models were used for the dipole resonance. Figures 1, 2, and 3 show the results of these theoretical form factors as a function of scattering angle. It was determined that a forward scattering angle of 75 degrees would be optimum for this experiment. At backward angles, greater than 90 degrees, transverse magnetic components would contribute significantly to the differential inelastic scattering cross section. These would complicate this study since it was desired to investigate, in particular, the dipole and quadrupole transition region of the spectrum. Calculations for the upper dipole transition which is due to the oscillation along the shorter axes, in ^{165}Ho indicated that this resonance would be sufficiently large in cross section to be readily detectible and not near a diffraction minimum if a scattering angle of 75 degrees were used. Also with increasing momentum transfer, produced by increasing the incident electron energy, the theory predicted a decrease in the relative strengths of the dipole resonance as compared to the

quadrupole resonance as seen in Figures 1 to 3. The selection of 75 degrees as the experimental scattering angle was not without some bias. This angle would allow direct comparison with the ^{197}Au and ^{208}Pb inelastic electron scattering results reported by Pitthan, *et. al.*, [Ref. 3].

A foil target of ^{165}Ho from Ventron Corporation was prepared and roll formed to a thickness of 145 mg/cm^2. The target foil was approximately one centimeter wide and three centimeters in length. A second foil of 259 mg/cm^2 was also prepared with similar dimensions. This size permitted the same foil sample to be used for all of the experimental runs since the focused beam area of the NPS linear accelerator is approximately 0.1 cm^2. The sample was placed in the target chamber and positioned for transmission geometry. (The electron linear accelerator facility of the Naval Postgraduate School is described by Warshawsky and Webber [Ref. 1].)

Four experimental runs were performed at incident electron energies of 60, 75, 90, and 105 MeV. All spectra except for 60 MeV investigated excitation energies to 40 MeV. The 60 MeV data was taken to 30 MeV excitation energy using the 259 mg/cm^2 target. The 75 MeV and 90 MeV experiments were done using both foils at each energy on separate occasions. The 105 MeV experiment used only the thinner target. It had been determined that using the thinner target reduced the background due to the radiative tail as is to be expected. In addition, the inelastic spectrum of the 75 MeV experiment with the 145 mg/cm^2 target was observed

twice with the same machine parameters to determine if there were significant differences in the spectra due to machine fluctuations during the course of the 48 hour data collection period. These experiments showed reproducible results confirming the stability of the experimental conditions. The count rates were maintained below 20 counts per second per channel to avoid losses due to electronic dead time of the triple coincidence ladder counting system. The total charge delivered by the beam was adjusted for each experiment to maintain less than three percent statistical uncertainty per channel. Table II lists the experimental conditions used for each run.

B. DATA ANALYSIS

The line shape fitting procedure developed by Darmstadt [Ref. 32] and the radiative tail calculations reported by Buskirk, *et. al.*, [Ref. 4] have been incorporated into a computer code called NAW [Ref. 33] for an IBM 360/67. This code is described and presented in Ferlic and Waddell [Ref. 2]. The entire inelastic spectrum including the resonances, radiation tail, and background were simultaneously fit assuming Breit-Wigner shapes for each resonance. Initial resonance energies and widths were chosen based on previously reported photoneutron data and from the general $A^{-1/3}$ behavior of giant multipole resonances [Ref. 3]. Resonance positions and widths were varied as input parameters while the computer code adjusted peak strengths and background parameters to obtain a best fit to the experimental data.

The code was subsequently modified to provide an option for maintaining a specific ratio of the two dipole resonance components. This was done to preserve the known giant dipole relative strength ratio as indicated in the theory and found by photonuclear experiments. (See Section II-D.)

The criteria used to determine a reasonable fit were as follows:

(1) The data and calculated spectrum should coincide visually on the superimposed spectrum plots.

(2) The χ^2 per degree of freedom should be less than one. The data is not strictly statistical because the detector momentum interval is larger than the momentum increment of the spectrometer field and hence correlations exist between energy bins.

(3) All observed resonances and widths should consistently fit each of the four spectra.

The 60 MeV spectrum is not considered as reliable as the other spectra even if these criteria were not apparently violated due to the use of the thicker target and the low incident electron energy. Here slightly different background parameters from those used at other energies were necessary to fit the data because of the differing experimental conditions. The higher background due to the radiative tail made extraction of the experimental inelastic form factors from the data difficult and somewhat arbitrary.

Figures 4 through 6 represent the experimental inelastic spectra corrected for spectrometer dispersion effects with

the fitted total background and the individual resonances superimposed. Figures 7 through 9 present corresponding spectra with the total background subtracted revealing the resonance structures and their features.

The areas under the inelastic resonances were calculated from the Breit-Wigner shapes and the ratio of each inelastic resonance area to the area of the elastic peak were presented in the NAW output with a statistical uncertainty. The elastic form factors for the experimental energies were determined using the phase shifted spherical wave calculations of Fisher and Rawitsher [Ref. 34]. The inelastic form factor could then be determined by the relation

$$|F_i|^2 = (A_i/A_{e1})|F_{e1}|^2. \qquad \text{(III-1)}$$

For these calculations the ground state charge distribution was assumed to be of the Fermi form

$$\rho_o(r) = 1 + e^{(r-c/4.4t)^{-1}} \qquad \text{(III-2)}$$

with c = 6.18 fm and t = 2.51 fm from Uhrhane, *et. al.*, [Ref. 12]. Table III presents the inelastic form factors obtained for the 75, 90, and 105 MeV experiments.

Table IV presents the transition probabilities that were obtained with the best fit resonance positions and widths. The values are reported for both conditions utilized within the computer code NAW - free fitting of all observed resonance strengths and free fitting of all strengths except that corresponding to the lower component of the dipole

transition. The strength of the latter was maintained at a fixed ratio to the upper component. The value of this ratio was determined from the (γ,n) experiments, using inelastic form factor calculations. For the E1 resonance the experimental strengths were determined for the surface oscillation (Goldhaber-Teller) model and the volume oscillation (Steinwedel-Jensen) model. Comparisons of these results with the appropriate energy weighted sum rule and single particle transition strengths are also made in Table IV.

C. ERROR ANALYSIS

Certain corrections must be made to the observed experimental electron scattering cross section. The observed area of both the elastic and inelastic lines must be increased since some of the electrons scattered at the corresponding energy suffer energy losses due to radiation during scattering, radiation and electronic collisions before and after scattering, and ionization straggling effects and hence are not counted at the proper energy [Ref. 16]. For the NAW code the radiation tail is calculated using the method described by Ginsberg and Pratt [Ref. 35] which was modified to use a phase shift calculation of the elastic scattering cross section to replace the original Born approximation cross sections [Ref. 4]. An analytic function is then used for the fit of the background due to the radiation tail and experimental processes. For this work an expression of the form

$$P_1 + P_2A + P_3\,RDT)\exp\frac{P_4}{E_o}(E_o-E_f) \qquad \text{(III-3)}$$

was used. E_o is the incident electron energy, E_f the energy of the scattered electron. $A = E_o - E_{fo}$ where E_{fo} is an expansion energy, and RDT is the calculated radiation tail. The P_i's are free parameters and are determined by the fitting routine.

Warshawsky and Webber [Ref. 1] describe the fractional error associated with the determination of the areas as a result of fractional errors in the Poisson counting statistics, variations in beam intensity during a run, and the error associated with the determination of the areas. Ferlic and Waddell [Ref. 2] investigated the energy and width relationships to the error in the determination of the area of Breit-Wigner shapes. They found contributions on the order of 20 percent in addition to the NAW statistical error. The total uncertainty would then be some function of these combined effects.

In addition a correction to the line shape due to a change in the inelastic form factor itself over the width of the resonance must be considered [Ref. 32]. Calculations of the theoretical inelastic form factors indicated a change in $|F_i|^2$ of several percent per MeV. For wide resonances the energy shift in the apparent resonance peak may be significant.

Repetition of the 75 MeV experiment during the same run with the machine parameter unchanged showed that current

control techniques maintain experimental conditions over the duration of the experiment. Hence, beam variations do not seem to be as large now as reported by Warshawsky and Webber [Ref. 1]. To provide an estimate of the true fractional error associated with each resonance would be most difficult. For this work an uncertainty of twice the statistical error computed by the NAW code is assumed for the data. This uncertainty is reported in Table III as a percentage error of the inelastic form factors obtained experimentally. The true uncertainty is at most this large and quite probably less.

Experimental Incident Energy (MeV)	Target Thickness (mg/cm^2)	Measured Incident Energy (MeV)	Elastic Peak Resolution (MeV)	q^2 (fm^2)	$\sigma_{el}/\sigma_{Mott}$ [Ref. 34]
60	259	60.77	.40	.137	2.6×10^{-1}
75	145	76.70	.42	.214	9.41×10^{-2}
	259	75.50	.40	.214	9.41×10^{-2}
90	145	90.85	.51	.309	5.49×10^{-2}
	259	90.11	.53	.309	3.49×10^{-2}
105	145	104.94	.58	.420	1.99×10^{-2}

Scattering angle was 75 degrees for all experiments.
Transmission geometry was used for target position.

Table II. Experimental Conditions.

Excitation Energy (MeV)	Incident Electron Energy					
	75 MeV	% Error	90 MeV	% Error	105 MeV	% Error
9.6	1.15×10^{-4}	34	8.32×10^{-5}	30	7.30×10^{-5}	20
11.5	5.92×10^{-4}	16	3.59×10^{-4}	12	2.49×10^{-4}	12
12.3	3.05×10^{-4}	38	9.56×10^{-5}	10	6.12×10^{-5}	30
15.8	6.62×10^{-4}	38	2.45×10^{-4}	10	1.53×10^{-4}	30
23.5	4.60×10^{-4}	50	1.78×10^{-4}	22	2.17×10^{-4}	24

Fixed Ratio of E1 Components

Table III. Inelastic Form Factors.

Multi-polarity	ΔT	E_x (MeV)	Γ_{nat} (MeV)	Calculated B(E ,q) (e^2MeV fm^2)	% EWSR [a]	SPU [b] ($e^2 fm^{2\lambda}$)	E_x ($A^{-1/3}$MeV)	B Values by Others
E0	0	9.6±.4	2.0±2	(1.29±0.8)x10^3 [c]	16±9	-	53	
E2	0	11.5±.4	4.0±1	(4.69±1.)x10^3 [d]	88±2	14.7	63	
E1	1	12.3 [g]	2.5 [g]	6.56 [d,f] 5.23 [e,f]	14 [f] 11 [f]	.8 [f] .6 [f]	67	19.5 [Ref. 9] 17.2 [Ref. 11]
E1	1	15.8 [g]	5.0 [g]	38.9±5. [d] 23.5±6. [e]	104±13 63±16	4.8 2.9	86	37.5 [Ref. 9] 30.4 [Ref. 11]
E2	1	23.5±1. [h]	7±1	(1.32±0.6)x10^3 [d]	34±14	4.1	133	

(a) Percentage of energy weighted sum rule given in Table I.
(b) B value in Weisskopf units given in Table I.
(c) Monopole matrix element in units of MeV-fm^4.
(d) Goldhaber-Teller model
(e) Steinwedel-Jensen model
(f) Upper limit
(g) Values from Ref. 11
(h) See section

Table IV. Reduced Transition Probabilities, free fitting of all peaks.

Table IV. Continued

Reduced Transition Probabilities, Fixed Ratio of E1 Components.

E0	0	9.8±.4	2.0±5	$(2.16\pm0.6)\times10^{3}$ [c]	27±7	-	53	
E2	0	17.5±.4	4.0±1	$(3.92\pm0.3)\times10^{3}$ [d]	73±6	12.3	63	
E1	1	12.3 [g]	2.5 [g]	14.5±3. [d] 9.0±2. [e]	30±5 19±4	1.8 1.1	67	19.5 [Ref. 9] 17.2 [Ref. 11]
E1	1	15.8 [g]	5.0 [g]	29.0±5 [d] 18.0±4	77±14 48±10	3.6 2.2	86	37.5 [Ref. 9] 30.4 [Ref. 11]
E2	1	23.5 [h]	7.0±1	$(1.90\pm0.8)\times10^{3}$	49±20	5.9	133	

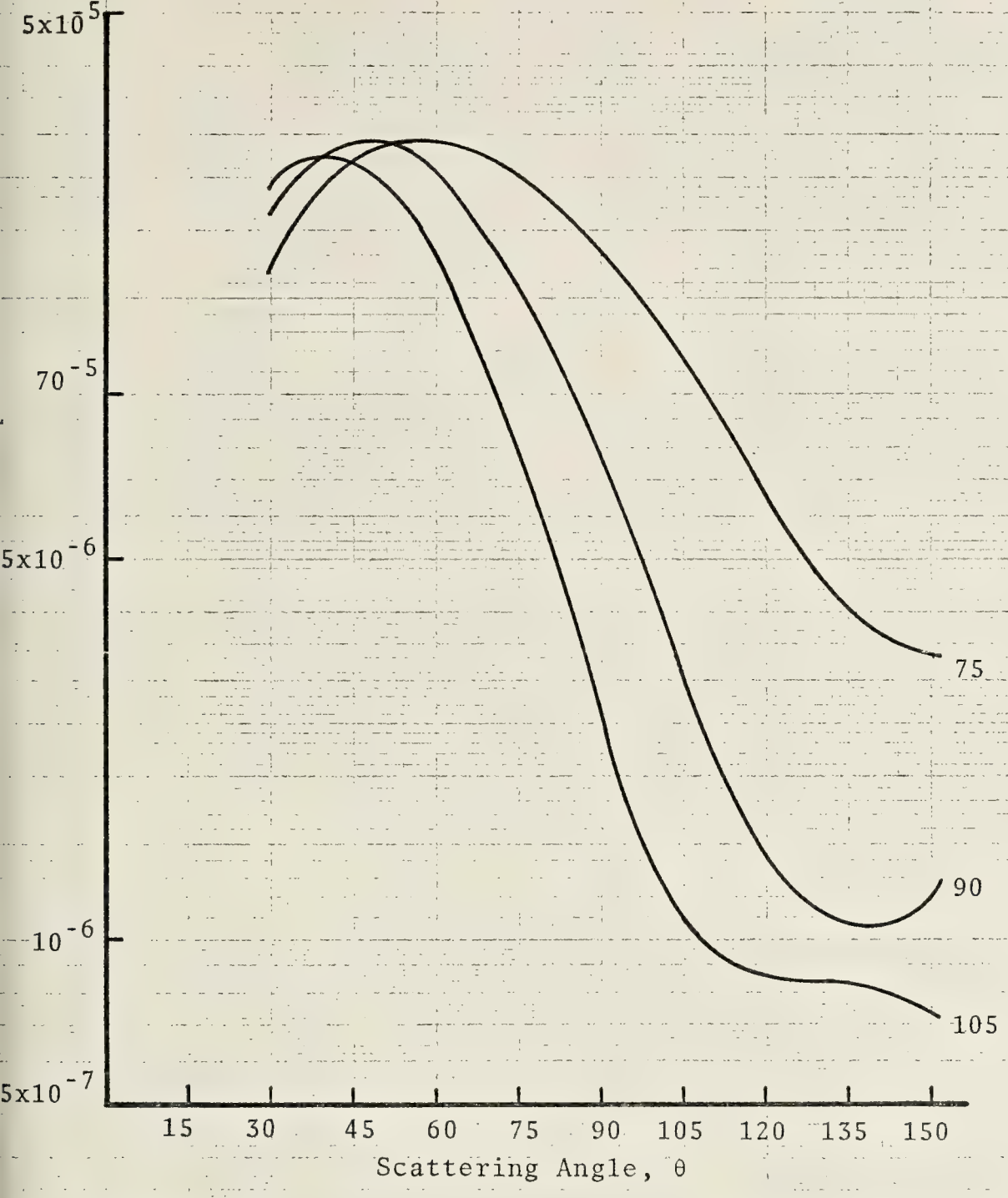

Figure 1. Inelastic form factor for E1 (upper component) transition predicted by Steinwedel-Jensen. Model for 75, 90, and 105 MeV incident electron energy.

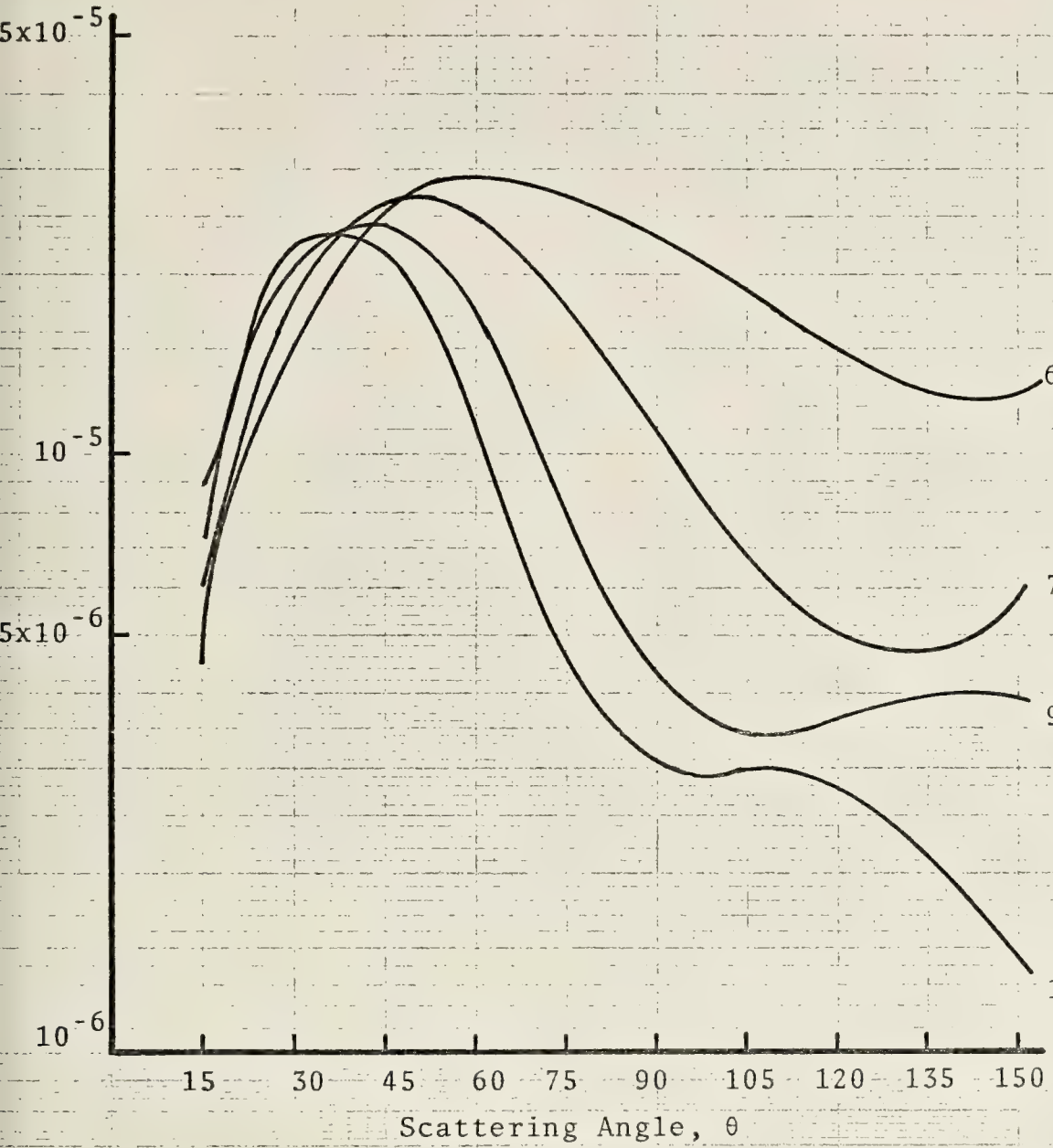

Figure 2. Inelastic form factor for E1 (upper component) transition predicted by Goldhaber-Teller Model for 60, 75, 90, and 105 MeV incident electron energy.

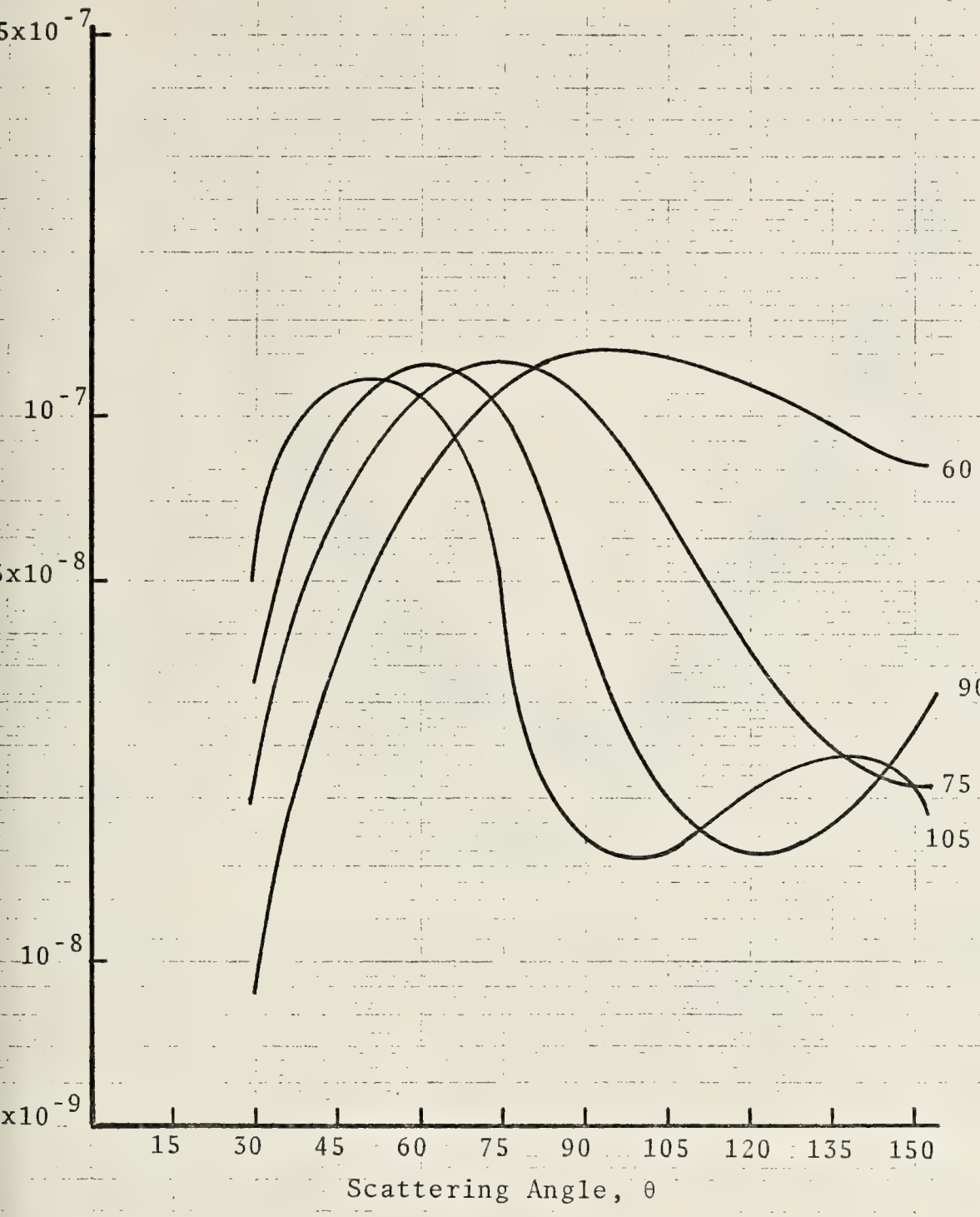

Figure 3. Inelastic form factor for E2 transition predicted by Goldhaber-Teller model for 60, 75, 90, and 105 MeV incident electron energy.

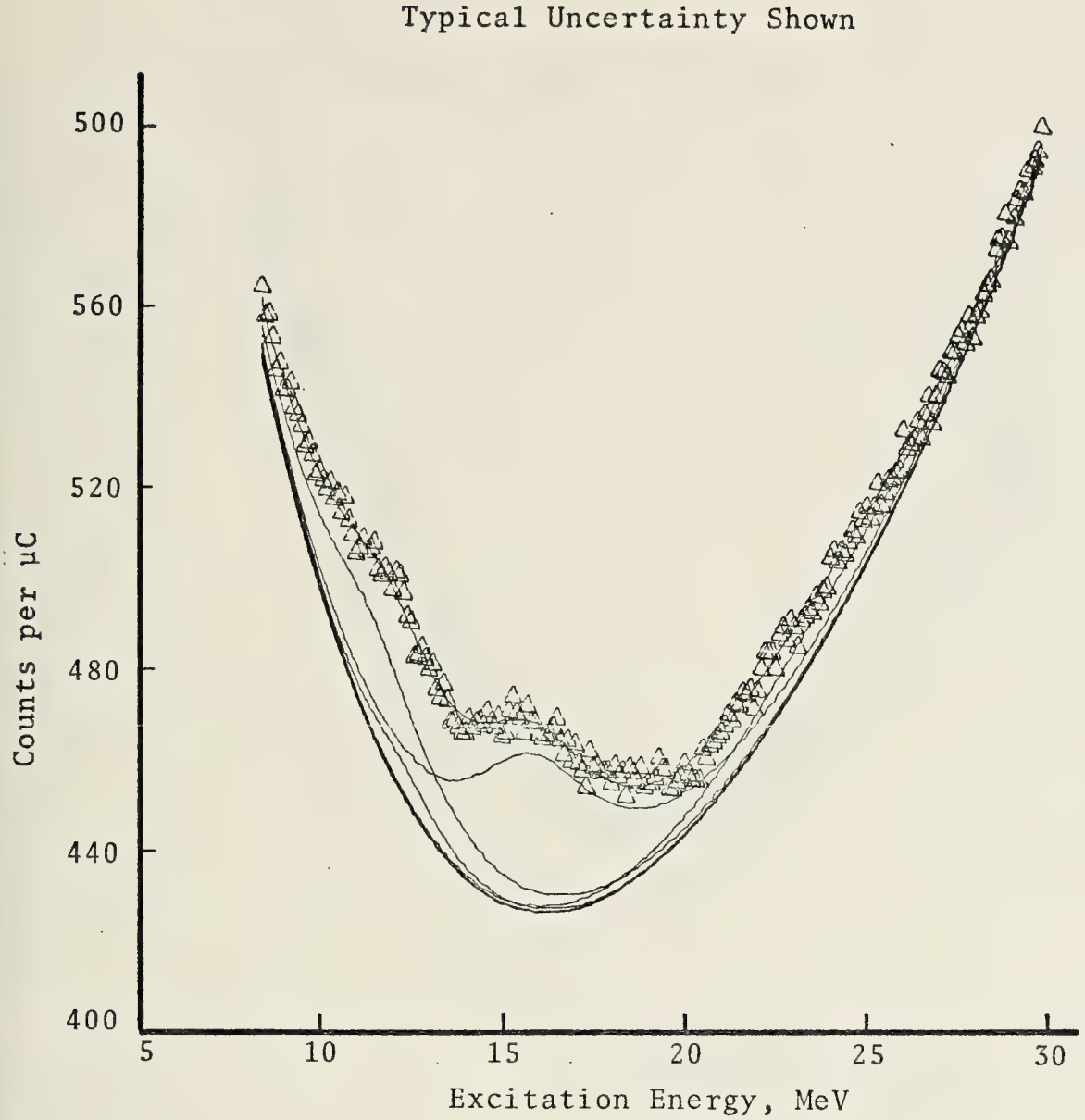

Figure 4. 75 MeV inelastic scattering spectrum with background.

Figure 5. 90 MeV inelastic scattering spectrum with background.

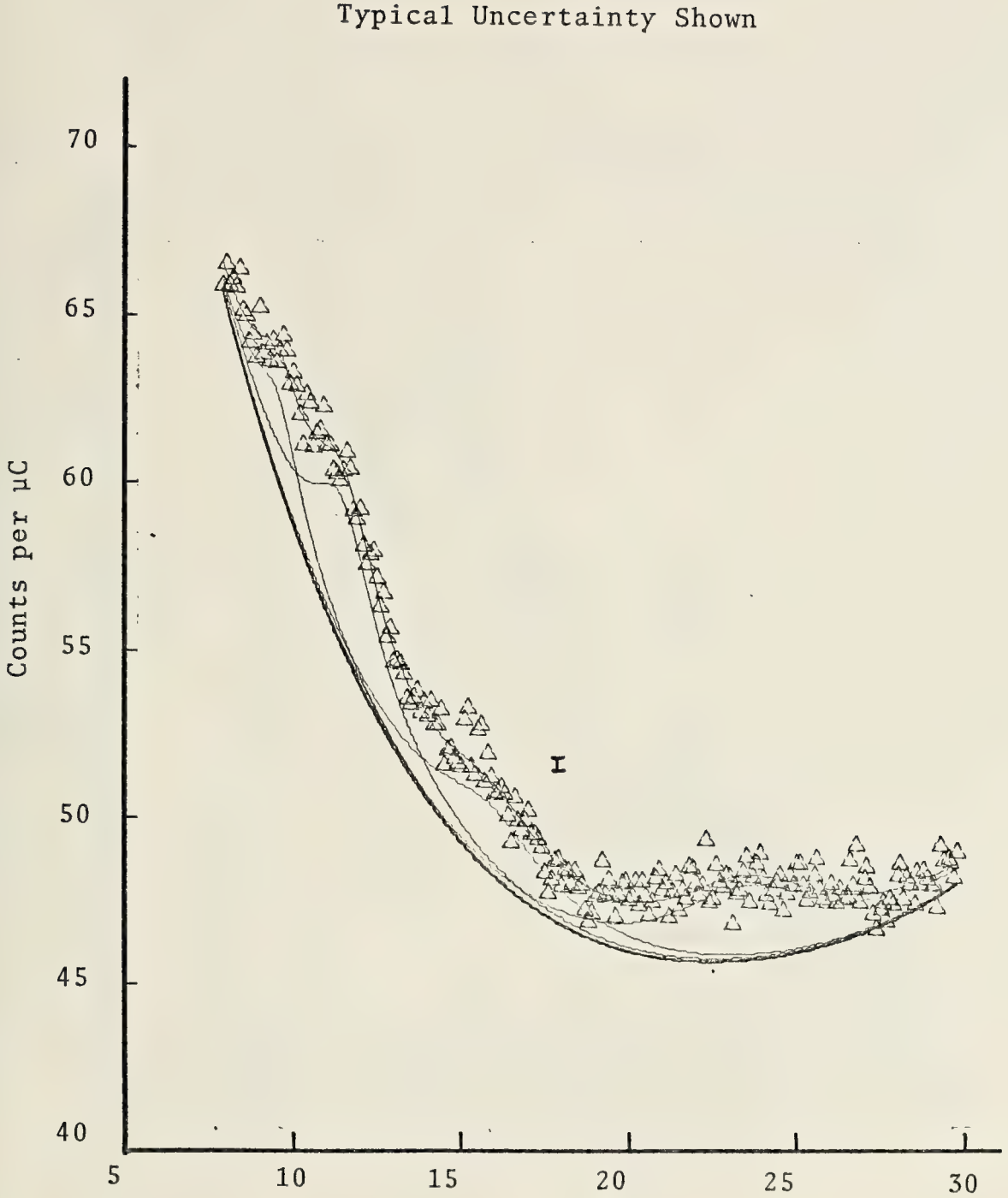

Figure 6. 105 MeV inelastic scattering spectrum with background.

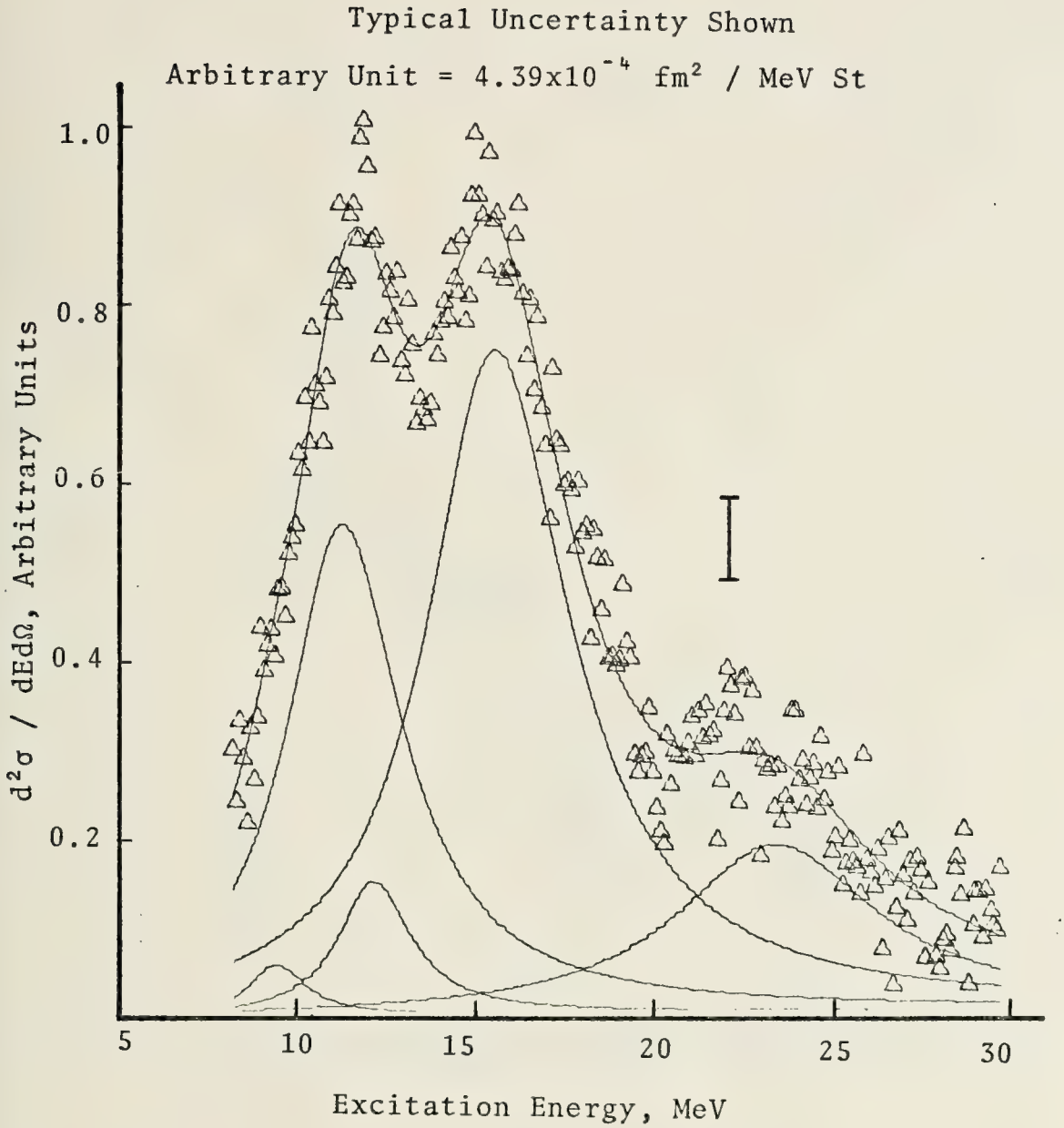

Figure 7. 75 MeV inelastic spectrum without background.

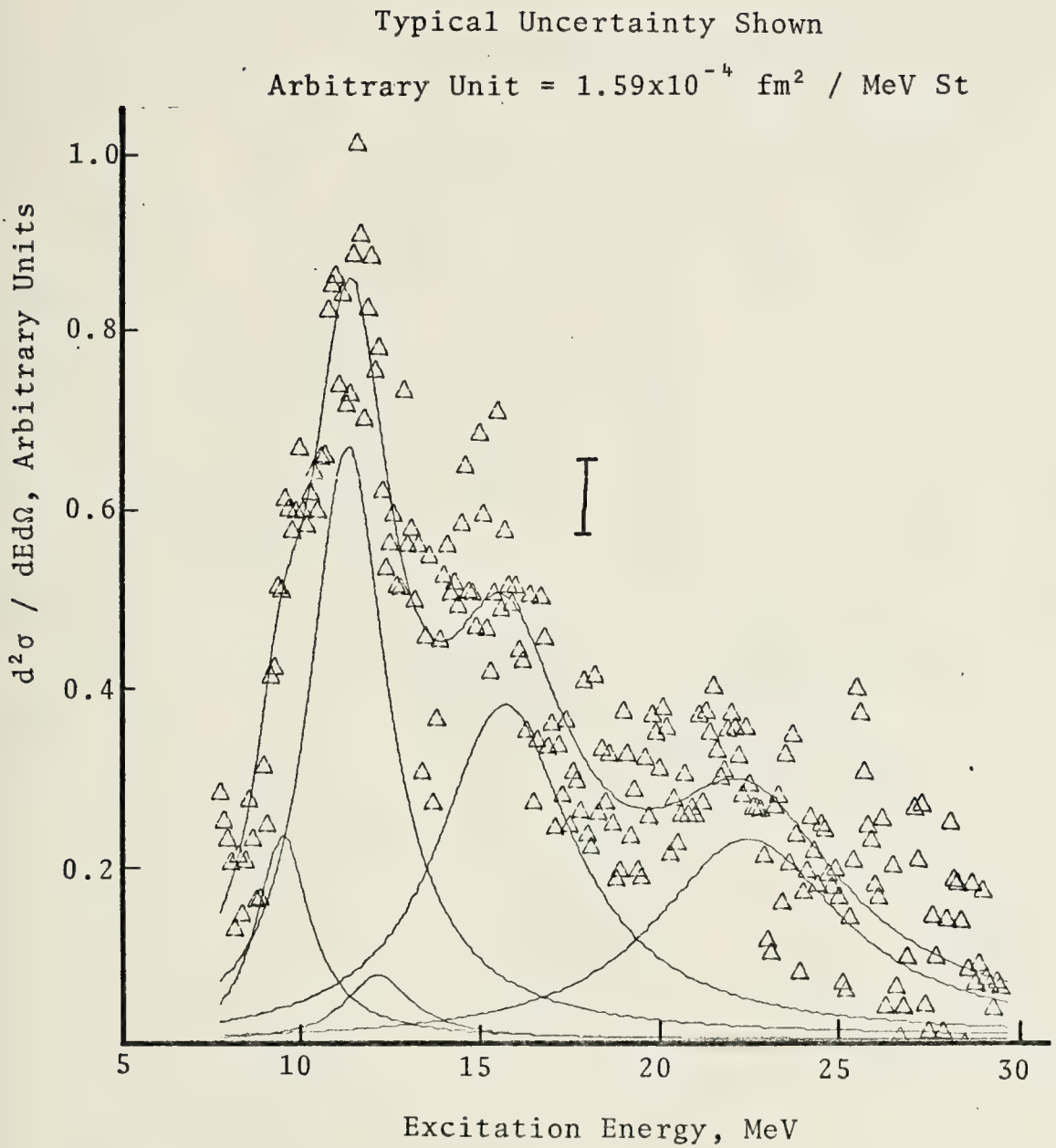

Figure 8. 90 MeV inelastic scattering spectrum without background.

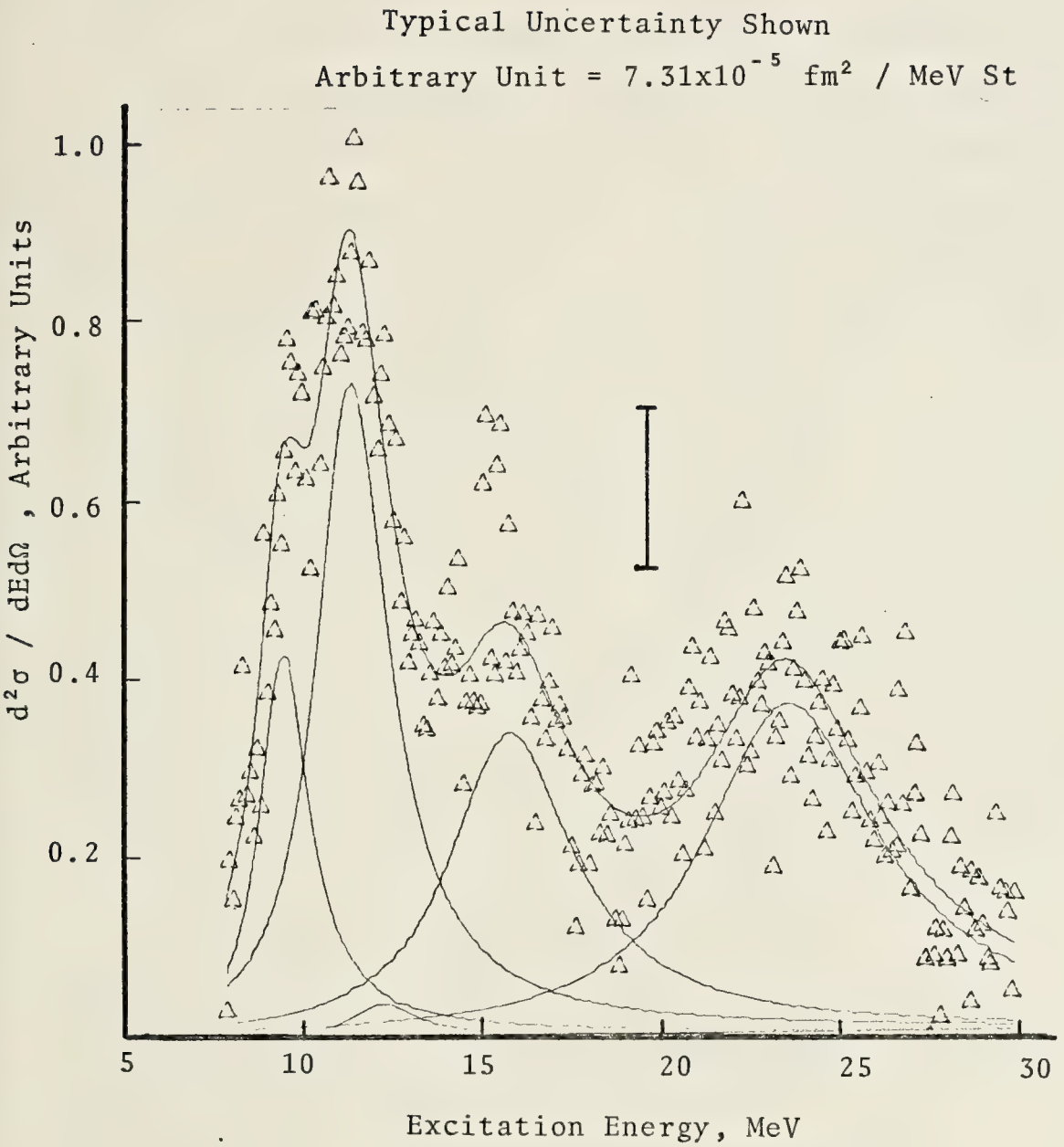

Figure 9. 105 MeV inelastic scattering spectrum without background.

IV. DISCUSSION

A. COLLECTIVE RESULTS

The data analysis indicates the presence of five resonances at excitation energies of 9.6, 11.5, 12.3, 15.8, and 23.5 MeV in the inelastic electron spectrum of ^{165}Ho. In the original data which extends to 40 MeV excitation energy, there exists the possibility of a sixth resonance at 33 MeV. However, it is not certain at this time if the peak is a true resonance or is generated by the experimental arrangement of the target chamber itself due to elastically scattered electrons passing through the metal of the spectrometer collimater. There are two reasons for accepting the resonance as real. First, in the energy loss experiments of Buskirk, *et. al.*, [Ref. 36], it was found that if the energy loss in lead is 6 MeV, the width of the distribution is 10 MeV. If it is now expected that the loss is over 30 MeV, the width would be over 30 MeV as compared to the 6 MeV width observed in lead. Since the observed structure has a preliminary fitted Breit-Wigner shape approximately 7 MeV wide, an energy loss mechanism for elastically scattered electrons does not seem to be the source. Second, an inelastic electron scattering experiment was performed with the spectrometer entrance collimator plugged and the resulting spectrum had no structure resembling the observed 33 MeV resonance. The exclusion of a 33 MeV resonance would not make significant changes in the transition

strengths reported here since the other resonances are all lower in excitation energy.

The conclusion that the other levels are true giant resonances is supported by the comparison of the transition strengths with the appropriate sum rule and the single particle transition strengths. In Table IV it can be seen that an appreciable percentage of the sum rule associated with each transition type is accounted for by the observed energy weighted B value. In addition, the B values are several Weisskopf units indicating that a collective response is being observed.

In Figures 8 and 9 it can be seen that the apparent heights of the resonances at 11.5 MeV and 23.5 MeV increase relative to the apparent height of the peak at 15.8 MeV as the incident electron energy increases. Recall that the scattering angle of 75 degrees was selected to observe the possible enhancement of the quadrupole resonance over the dipole for increasing momentum transfer. Since the 12.3 MeV and 15.8 MeV resonances are known to be dipole resonances from the photoneutron work with ^{165}Ho, the first assessment of the 11.5 MeV and 23.5 MeV resonances is that they are quadrupole resonances.

For each experiment the overall fit was improved by the modification to the computer code NAW as described in Section III-B. Resolution of the two resonances at 11.5 MeV and 12.3 MeV was not sufficient due to the large width of both peaks. In the initial free fitting attempts it was found that the 11.5 MeV resonance was enhanced and

that only a relatively small resonance at 12.3 MeV was required to meet the criteria of a good fit. This caused the calculated B values for the 12.3 MeV resonance to be much smaller than the B values of the photoneutron work (Table IV). Also the assumed lower E1 resonance component had B values in Weisskopf units of approximately unity. This would indicate a single particle scattering effect. Fitting with a constraint on the ratio of the strengths of the lower and upper dipole resonances gave better agreement between measured and calculated form factors.

B. RESONANCES AND CHARACTERISTICS

Each of the observed resonances is discussed in this section.

1. 9.6 MeV

An E0 isoscalar resonance at 53 $A^{-1/3}$ was reported previously at this facility [Ref. 3] in ^{197}Au and ^{208}Pb. This would correspond to an excitation energy of 9.6 MeV in ^{165}Ho. The existence of a resonance in this region is clearly seen in the 105 MeV experimental data in Figure 9. The calculated magnitude of the matrix element of an assumed monopole resonance would exhaust 28 percent of the monopole sum rule.

2. 11.5 MeV

The resonance at 63 $A^{-1/3}$, 11.5 MeV for ^{165}Ho, is now generally believed to be the isoscalar quadrupole giant resonance [Ref. 3]. As noted in Table IV the energy weighted

observed strength exhausts 73 percent of the quadrupole sum rule for the natural width of the resonance assumed. However, fitting attempts were made with the width of this E2 between 2.9 MeV and 4.5 MeV and the χ^2 obtained in each was approximately the same, but with rather different percentages of the sum rule. The strength of the resonances at 9.6 MeV and 15.8 MeV were not significantly affected in these different iterations. A relatively wide resonance would, of course, indicate unresolved quadrupole splitting. The uncertainty in the observed width precludes answering that question based on this data.

3. 12.3 MeV

This is known to be the lower excitation energy of the giant dipole resonance for the deformed ^{165}Ho nucleus [Refs. 9, 10, and 11]. It was found that the excitation energy and natural width as reported by Berman, *et. al.*, [Ref. 11] in the photonuclear work for the resonance at 12.3 MeV fit remarkably well to the observed experimental data from inelastic electron scattering. This E1 resonance was fitted by a fixed ratio of its inelastic form factor to that of the resonance at 15.8 MeV, hence its reduced transition strength is a function of the strength observed for the upper, better visible, component of the dipole resonance. These strengths are discussed in the next section An assignment of an E1 isovector multipolarity based on the results of the photoneutron data and of this work is considered well supported.

4. 15.8 MeV

This is the predicted partner in the dipole resonance splitting of the deformed nucleus ^{165}Ho [Refs. 9, 10 and 11]. The energy and width reported by Berman, *et. al.*, [Ref. 11] were used in the initial fit and were found to not vary significantly in subsequent trials. The experimental inelastic form factors shown in Figure 10 can be described reasonably well with either model. The close agreement for the upper component of the dipole resonance is considered valid evidence that the observed splitting is a real effect in the prolate spheroid, ^{165}Ho. Comparison of the energy weighted sums provides some model selectivity. The Goldhaber-Teller model exhausts 107 percent of the E1 resonance sum rule with the 12.3 MeV and 15.8 MeV combined. For the Steinwedel-Jensen model the two comprise only 67 percent of the sum rule. The strengths as reported by the Saclay group [Ref. 9] comprise 120 percent of the sum rule, while the values reported by Berman, *et. al.*, [Ref. 11], exhausts 106 percent of the sum. Thus the Goldhaber-Teller model is favored by this data in comparison with the results of the photoneutron work. The assignment of an E1 isovector to this resonance and the 12.3 MeV resonance is consistent with previous work [Refs. 3, 9, 10, and 11].

5. 23.5 MeV

This resonance has not been reported previously. It appears strongly in the 105 MeV experimental data, Figure 9. Berman, *et. al.*, [Ref. 11] noted some structure in the photoneutron work of ^{165}Ho in this excitation region. The

calculated B value for this work exhausts 49 percent of the energy weighted sum rule for an E2 isovector resonance. In the ^{197}Au and ^{208}Pb work [Ref. 3] the isovector quadrupole was reported at 133 $A^{-1/3}$. This would be approximately 24 MeV for ^{165}Ho. In addition an E2 assignment would be consistent with the structure reported by Berman, *et. al.*, [Ref. 11]. However, the data because of its relatively large width of 7 MeV, indicate a possible splitting of the isovector E2 resonance in several levels, which makes a fit by one Breit-Wigner resonance quite inadequate.

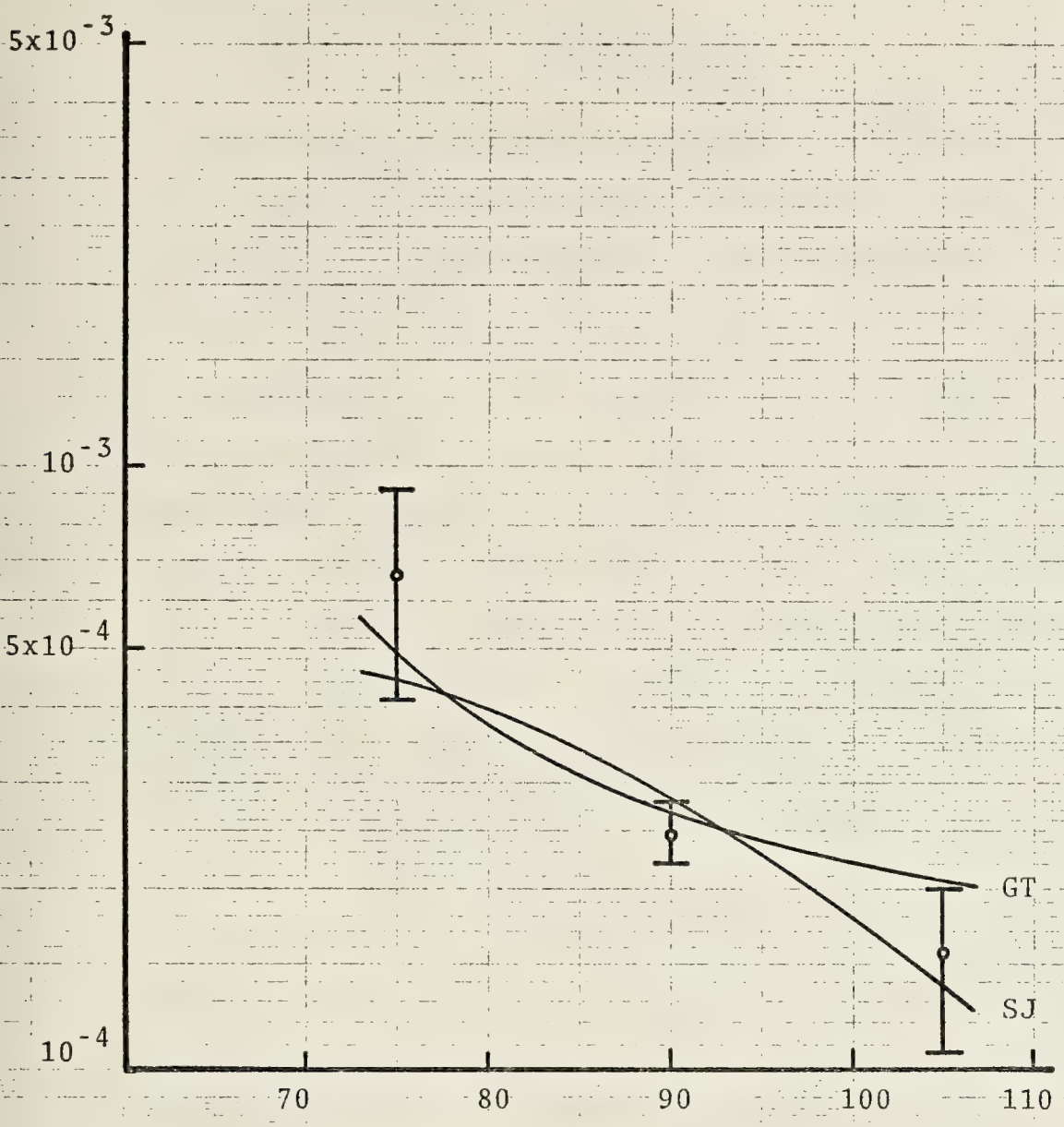

Figure 10. Experimental inelastic form factor for E_x = 15.8 MeV compared with Goldhaber-Teller (GT) model and Steinwedel-Jensen (SJ) model.

V. CONCLUSIONS

Giant multipole resonances studied by inelastic electron scattering in ^{165}Ho indicate five resonances in the excitation range of 5 MeV to 30 MeV. These resonances occur at 9.6, 11.5, 12.3, 15.8, and 23.5 MeV. The 12.3 MeV and 15.8 MeV resonances have been reported in the photoneutron work and are known to be electric dipole. In spherical nuclei these dipole resonances are threefold degenerate in energy, whereas for prolate spheroids such as ^{165}Ho the observed single resonance is split into two separately resolved resonances. There exists a correlation between the transition strengths of the two resonances which are found to be in the ratio of 1:2 for the lower energy resonance in respect to the upper component.

The experiments fit E1 form factors for either the Goldhaber-Teller or Steinwedel-Jensen models. However, only the strength calculated from the Goldhaber-Teller model agrees with the sum rule and (γ,n) experiments.

In this series of experiments a significant difference in technique compared to most previous experiments consisted in the use of one scattering angle and various energies. The advantages and disadvantages of this procedure can be summaried as follows:

1. No magnetic transitions appeared in the excitation energy range of 5 to 15 MeV, which includes the E0, E2 and E1 transitions.

2. The resulting variation of the momentum transfer q is small, so no diffraction minima are included. If nothing were known about these resonances, these experiments alone would not decide between E1 and E2 assignments as conclusively as the other experiments.

The giant quadrupole which appears as a general feature in heavy nuclei [Ref. 3] is observed at 11.5 MeV for ^{165}Ho. One objective was to choose a range of momentum transfer such that the E2 resonances would be enhanced relative to the E1 resonance. This enhancement occurred in the 105 MeV run, in which the E2 is about twice as large as the lower E1. The width of the E2 was not decisively determined because of the presence of the 9.6 and 12.3 MeV levels. Width from 2.9 to 4.0 MeV fit reasonably well, with 4.0 MeV favored. Thus the expected splitting or broadening of the E2 resonance in the deformed nucleus is not definite. The surface oscillation model is strongly favored. The additional E2 isovector resonance at 23.5 MeV has not been previously reported in ^{165}Ho although the general feature was reported by Pitthan, *et. al.*, [Ref. 3] in gold and lead at 133 $A^{-1/3}$. An assumed monopole resonance at 9.6 MeV was found in the experimental data which corresponds closely with the 53 $A^{-1/3}$ feature.

Using the information for the inelastic form factors, the corresponding reduced transition probabilities and comparisons with the energy weighted sum rules it was possible to determine multipolarity of the resonances. Good agreement

was found between this experiment and the previous gold and lead experiments in terms of the general $A^{-1/3}$ relations for the various resonances. The excitation energy, width, and multipolarity assignments made in this work are presented in summary in Table V along with the results reported earlier for ^{197}Au and ^{208}Pb.

Table V. Giant Resonances.

E_x $A^{-1/3}$MeV	E_x (MeV)	Γ_{nat} (MeV)	Multipolarity Assumed
	^{165}Ho		
53	9.6	2.0±5.	E0 or E2 isoscalar
63	11.5	4.0±1.	E2 isoscalar
67	12.3[a]	2.5[a]	E1 isovector
86	15.8[a]	5.0[a]	E1 isovector
133	23.5	7.0±1	E2 isovector
	^{197}Au		
53	9.2	2.2±0.5	E0 isoscalar
63	10.8	2.9±0.2	E2 isoscalar
81	14.0	4.5±0.2	E1 isovector
133	23.0	7 ± 1	E2 isovector
	^{208}Pb		
53	8.9	1.8±0.5	E0 isoscalar
63	10.5	2.8±0.3	E2 isoscalar
81	13.6	3.9±0.1	E1 isovector
133	22.5	5 ± 1	E2 isovector

[a][Ref. 11]

LIST OF REFERENCES

1. Warshawsky, A. S. and Webber, M. W., Jr., Naval Postgraduate School Thesis (1973).

2. Ferlic, K. P. and Waddell, R. D., Naval Postgraduate School Thesis (1974).

3. Pitthan, R., Buskirk, F. R., Dallay, E. B., Dyer, J. N., Maruyama, X. K., Phys. Rev. Lett. 33, 849, (1974).

4. Buskirk, F. R., Graf, H. D., Pitthan, R., Theissen, H., Titze, O., Walcher, T., Phys. Rev. Lett., 42B, 194 (1972).

5. Fuller, E. G., Petree, B., Weiss, M. S., Phys. Rev. 112, 554 (1958).

6. Fuller, E. G. and Hayward, E., Nucl. Phys. 30, 613, (1972).

7. Bramblett, R. L., Caldwell, J. T., Auchampaugh, G. F., Fultz, S. C., Phys. Rev. 129, 2723 (1963).

8. Safrata, R. S., McCarthy, J. S., Little, W. A., Yearian, M. R., Hofstadter, R., Phys. Rev. Lett. 18, 667 (1967).

9. Bergère, R., Beil, H., Veyssière, A., Nucl. Phys. A121, 463 (1968).

10. Kelly, M. A., Berman, B. L., Bramblett, R. L., Fultz, S. C., Phys. Rev. 179 (1969).

11. Berman, B. L., Kelly, M. A., Bramblett, R. L., Caldwell, J. T., Davis, H. S., Fultz, S. C., Phys. Rev. 185 (1969).

12. Uhrhane, F. J., McCarthy, J. S., Yearian, M. R., Phys. Rev. Lett. 26, 578 (1971).

13. Berman, B. L., Atlas of Photoneutron Cross Sections Obtained with Monoenergetic Photons, 2nd ed., Lawrence Livermore Laboratory, UCRL-75694 (1974).

14. Goldhaber, M. and Teller, E., Phys. Rev. 74, 1046 (1948).

15. Steinwedel, H. and Jensen, J. H. D., Z. Maturforsch A5, 413 (1950).

16. Überall, H., Electron Scattering From Complex Nuclei, Academic Press, New York (1971).

17. Mott, N. F. Proc. Roy. Soc. (London) A124, 425 (1929), as reprinted in Hofstader, R. Electron Scattering and Nuclear Structure, Benjamin, New York (1963).

18. Theissen, H., Spectroscopy of Light Nuclei by Low Energy (< 70MeV) Inelastic Electron Scattering, Institut für Technische Kernphysik der Technischen Holschule, Darmstadt (1972).

19. Ziegler, J. F., The Calculation of Inelastic Electron Scattering by Nuclei (1967): available from the Clearinghouse for Federal Scientific and Technical Information, National Bureau of Standards, U.S. Department of Commerce, Springfield, Va., 22151 under publication number Yale 2726E-49.

20. Adler, K., Bohr, A., Hans, T., Mottleson, B., Winther, A., Rev. Mod. Phys. 28, 432 (1956).

21. Skorka, S. J., Hertel, J., Retz-Schmidt, T. W., Nucl. Data A 2, 347 (1966).

22. Nathan, O. and Nilsson, S. G., in Alpha, Beta, and Gamma-ray Spectroscopy, ed. by K. Siegbahn, North-Holland Publishing Company, Amsterdam (1966).

23. Ferrell, R. A., Phys. Rev. 101, 1631 (1957).

24. Warburton, E. K. and Weneser, G., in The Role of Isospin in Electromagnetic Transitions, ed. by Wilkinson, D. H., North-Holland Publishing Company (1969).

25. Danos, M., Nucl. Phys. 5, 23 (1958).

26. Hayward, E., Photonuclear Reactions, Physics Part IV Lecture Notes. School of Physics, University of Melbourne, Australia (1969).

27. Okamoto, K., Phys. Rev. 110, 143 (1958).

28. Schiff, L. I., Phys. Rev. 96, 765 (1954).

29. Ligensa, R., Greniner, W., Danos, M., Phys. Rev. Lett. 16B, 535 (1966).

30. Pitthan, R. and Walcher, T., Phys. Rev. Lett. 368, 563 (1971).

31. Nagao, M. and Torizuka, V., Phys. Rev. Lett. 30, 1068 (1973).

32. Pitthan, R., Dissertation, Institut für Kernphysik der TH, Darmstadt (1972): unpublished.

33. Titze, O., Technical Report, Institut für Kernphysik der TH, Darmstadt (1967): unpublished.

34. Fisher, C. R. and Rawitsher, G. A., Phys. Rev. 135, B377 (1964).

35. Ginsberg, A. and Pratt, R., Phys. Rev. 134, B773 (1964).

36. Buskirk, F. R., Dyer, J. N., Marayama, X. K., Woehler, K. E., Z. Physik, accepted for publication.

INITIAL DISTRIBUTION LIST

		No. Copies
1.	Defense Documentation Center Cameron Station Alexandria, Virginia 22314	2
2.	Library, Code 0212 Naval Postgraduate School Monterey, California 93940	2
3.	Physics Library, Code 61 Department of Physics and Chemistry Naval Postgraduate School Monterey, California 93940	1
4.	Professor F. R. Buskirk, Code 61Bs Department of Physics and Chemistry Naval Postgraduate School Monterey, California 93940	2
5.	Professor X. K. Maruyama, Code 61Mp Department of Physics and Chemistry Naval Postgraduate School Monterey, California 93940	2
6.	Professor W. R. Pitthan, Code 61Pt Department of Physics and Chemistry Naval Postgraduate School Monterey, California 93940	2
7.	LT Gerald L. Moore, USN Class 1-75 Naval Destroyer School Newport, Rhode Island 02840	1

Thesis
M767 Moore
c.1
157048
Electroexcitation of giant resonances between 5 MeV and 30 MeV excitation energy in ^{165}Ho.